Magnetoelectric properties of epitaxial Fe3O4 thin films on (011) PMN-PT piezosubstrates

Alexander Tkach, Mehrdad Baghaie Yazdi, Michael Foerster, Felix Büttner, Mehran Vafaee, Maximilian Fries, Mathias Kläui

Angaben zur Veröffentlichung / Publication details:

Tkach, Alexander, Mehrdad Baghaie Yazdi, Michael Foerster, Felix Büttner, Mehran Vafaee, Maximilian Fries, and Mathias Kläui. 2015. "Magnetoelectric properties of epitaxial Fe3O4 thin films on (011) PMN-PT piezosubstrates." *Physical Review B* 91 (2): 024405. https://doi.org/10.1103/physrevb.91.024405.

Magnetoelectric properties of epitaxial Fe_3O_4 thin films on (011) PMN-PT piezosubstrates

Alexander Tkach,[1,2] Mehrdad Baghaie Yazdi,[3] Michael Foerster,[1,4] Felix Büttner,[1,5] Mehran Vafaee,[1,3] Maximilian Fries,[3] and Mathias Kläui[1]

[1]*Institute of Physics, Johannes Gutenberg University, Staudingerweg 7, 55128 Mainz, Germany*
[2]*Department of Materials and Ceramic Engineering, CICECO, University of Aveiro, 3810-093 Aveiro, Portugal*
[3]*Institute of Materials Science, Technical University of Darmstadt, Petersenstrasse 23, 64287 Darmstadt, Germany*
[4]*ALBA Synchrotron Light Source, Carretera BP 1413, km. 3.3, Cerdanyola del Valles 08290, Spain*
[5]*Institut of Optics and Atomic Physics, Technical University of Berlin, Strasse des 17 Juni 135, 10623 Berlin, Germany*

(Received 2 February 2014; revised manuscript received 17 December 2014; published 7 January 2015)

We determine the magnetic and magnetotransport properties of 33 nm thick Fe_3O_4 films epitaxially deposited by rf-magnetron sputtering on unpoled (011) $[PbMg_{1/3}Nb_{2/3}O_3]_{0.68} - [PbTiO_3]_{0.32}$ (PMN-PT) substrates. The magnetoresistance (MR), as well as the magnetization reversal, strongly depend on the in-plane crystallographic direction of the epitaxial (011) Fe_3O_4 film and strain. When the magnetic field is applied along [100], the magnetization loops are slanted and the sign of the longitudinal MR changes from positive to negative around the Verwey transition at 125 K on cooling. Along the $[01\bar{1}]$ direction, the loops are square shaped and the MR is negative above the switching field across the whole temperature range, just increasing in absolute value when cooling from 300 K to 150 K. The value of the MR is found to be strongly affected by poling the PMN-PT substrate, decreasing in the [100] direction and slightly increasing in the $[01\bar{1}]$ direction upon poling, which results in a strained film.

DOI: 10.1103/PhysRevB.91.024405 PACS number(s): 75.30.Gw, 75.47.Lx, 75.70.−i

I. INTRODUCTION

Artificial multiferroics, consisting of ferro(i)magnetic and ferroelectric components, attract much interest, because voltage-driven control of magnetization promises lower energy consumption and better scaling than conventional magnetization manipulation involving electrical currents in electronic devices [1]. The electric field control of the magnetization in artificial multiferroic structures can be mediated by three main mechanisms: strain, exchange bias, and charge due to ferroelectric polarization reversal [1]. The strain-mediated magnetoelectric coupling is related to magnetoelastic properties of the magnetic film and piezoelectric response of the ferroelectric substrate and has been shown to be useful to manipulate magnetization for instance in Ni [2]. Interesting materials beyond previously used 3d metals include magnetite (Fe_3O_4), possessing large magnetostriction [3], which undergoes a paramagnetic to ferrimagnetic transition at ∼848 K and a charge-ordering Verwey transition at $T_V \sim$ 125 K, below which it becomes progressively insulating [4]. To generate strain, one can use $[Pb(Mg_{1/3}Nb_{2/3})O_3]_{0.68} - [PbTiO_3]_{0.32}$ (PMN-PT), which is a relaxor ferroelectric with high piezoelectric coefficients below 400 K [5]. Under an out-of-plane electric field, the (011)-oriented PMN-PT single crystal generates opposite strain in the orthogonal in-plane x [100] and y $[01\bar{1}]$ directions [6]. Due to the resulting effective uniaxial strain, a strong electric field tuning of the magnetic properties was observed in spin-spray deposited polycrystalline Fe_3O_4 films on (011) PMN-PT [7]. More recently, 55 nm thick Fe_3O_4 films were reported to be grown epitaxially on (011) $[Pb(Mg_{1/3}Nb_{2/3})O_3]_{0.71} - [PbTiO_3]_{0.29}$ by molecular beam epitaxy (MBE), demonstrating a nonvolatile resistance switching [8]. Moreover, an 8 K shift of the Verwey transition temperature from 125 K to 117 K, induced by poling the PMN-PT substrate under 10 kV/cm electric field, was reported from the temperature dependence of the Fe_3O_4 film resistance, measured in the [100] direction. The magnetoresistance (MR) measured along [100] in magnetic fields up to 6 T was also found to be smaller in the poled sample compared to the unpoled one below 180 K [8]. As for the use in devices, the readout has to be based on transport, and the detailed magnetotransport needs to be understood. However, no magnetotransport measurements for Fe_3O_4 films on (011) PMN-PT in $[01\bar{1}]$ or other directions have been reported and no relation to the magnetic properties along different crystallographic orientations has been established. So in order to use this highly spin-polarized and piezoelectric materials heterostructure a complete characterization of this promising system including the magnetotransport response is a key necessity.

In the current work, we study the magnetotransport and magnetic properties of 33 nm thick Fe_3O_4 films epitaxially deposited on $[Pb(Mg_{1/3}Nb_{2/3})O_3]_{0.68} - [PbTiO_3]_{0.32}$ by rf-magnetron sputtering systematically to determine their relation to the in-plane crystallographic orientation. We show that the coercive field and the MR response are very different for [100] and $[01\bar{1}]$ directions highlighting the importance of the magnetocrystalline anisotropy. An orientation-dependent modification of the MR in Fe_3O_4 is observed after poling PMN-PT under 4 kV/cm electric fields, showing that strain can be used to manipulate the magnetotransport and magnetic materials properties.

II. EXPERIMENT

The thin films of magnetite Fe_3O_4 were deposited onto single-crystalline unpoled (011) PMN-PT substrates heated to 450 °C by rf-magnetron sputtering of the iron target in a 98% Ar + 2% O_2 mixture [9]. The thickness of the films deduced by x-ray reflectometry is $t = 33$ nm, while x-ray diffraction analysis confirms the epitaxial growth mode. An (011) orientation of the magnetite film with out-of-plane lattice

parameter of $a = 8.31$ Å and without secondary phases was verified by standard θ-2θ scan. A φ scan around the (404) peak of magnetite, with the corresponding substrate peak, revealed the expected twofold symmetry in both cases, confirming that the Fe_3O_4 film has grown epitaxially following the crystallographic symmetry of the PMN-PT substrate. Additionally, the Verwey transition temperature T_V was deduced from the transport measurements to be above 125 K, confirming the high quality and proper stoichiometric ratio of the obtained magnetite films.

Magnetoresistance measurements were performed in a van der Pauw configuration with contacts in the four corners of the sample, using a system electrometer (Keithley 6514) as a current source and a 6.5 digit multimeter (Agilent 34411A) as a voltmeter. The magnetic field up to 0.3 T was generated by an electromagnet (GMW 3470) powered by a bipolar power supply (Kepco BOP 36-6M). All the MR measurements in this work were conducted by applying the magnetic field in the film plane. A sample rotator was used to measure the MR as a function of the angle between the direction of magnetic field and current at room temperature, whereas low-temperature measurements and poling of the PMN-PT substrate were done in a He cryostat (Oxford Instruments, MicrostatHe).

The same electromagnet, power supply, and sample rotator were used for magneto-optic Kerr effect (MOKE) measurements. A HeNe laser system (CVI Melles Griot) with a wavelength of $\lambda = 632.8$ nm and an output power of 5 mW produces a nearly linearly polarized beam passing through a Glan-Thompson polarizer (Thorlabs) with an extinction coefficient of 10^{-5}, which produces a high degree of polarization. The beam reflected from the sample is periodically modulated at 50 kHz between left and right circularly polarized light by a photoelastic modulator (Hinds Instruments PEM-100). The modulation signal is used as a reference signal for a lock-in amplifier (Signal Recovery 7225 DSP). The beam is transmitted through an analyzer (polarizer with the transmission axis rotated by 45°) and is finally detected by a photosensitive fast-responding diode (Hinds Instruments DET-200). The magnetization loops obtained by MOKE were normalized to those obtained by a superconducting quantum interference device (SQUID) magnetometer (Quantum Design MPMS-XL) along the [100] and [01$\bar{1}$] directions after subtraction of the substrate diamagnetic component.

III. RESULTS AND DISCUSSION

Figure 1 shows the magnetization loops of magnetite films on (011) PMN-PT, obtained at room temperature by the SQUID technique along the [100] and [01$\bar{1}$] directions [Fig. 1(a)] and by the MOKE technique along different directions and complemented by the SQUID along [100] [Fig. 1(b)] in order to investigate the magnetic anisotropy. Clear hysteresis is observed indicating the ferrimagnetic state of the films at room temperature. However, while in the [01$\bar{1}$] direction the loop is square shaped, it is slanted and slim in the [100] direction, indicating a hard-axis behavior. The hard-axis loop closes and the magnetization becomes constant at an anisotropy field H_a with an absolute value of ~0.3 T, as shown in Fig. 1(a). The magnetization curves were also

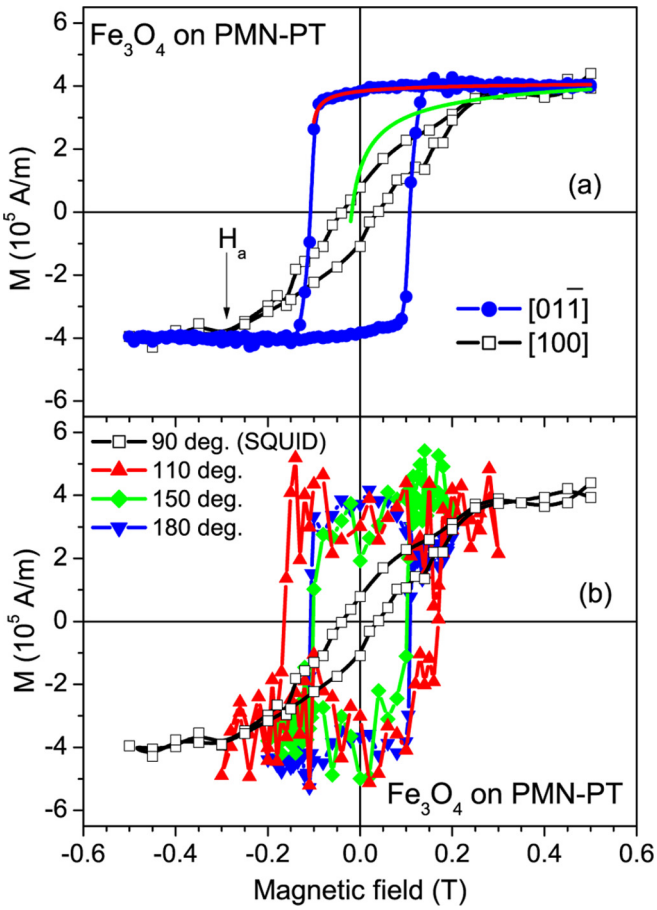

FIG. 1. (Color online) Room-temperature magnetization loops of the Fe_3O_4 film on (011) PMN-PT, measured (a) along the [100] (open squares) and [01$\bar{1}$] (solid circles) directions by the SQUID with their fits (red and green solid lines) to Eq. (1) and (b) along different in-plane directions (solid squares) by the MOKE technique (the 90° loop, corresponding to the [100] direction, is measured by SQUID). Lines connecting points are a guide to the eye.

analyzed using a simplified equation,

$$M(H)/M(\infty) = 1 - qH^{-0.5}, \quad (1)$$

where the parameter q indicates the difficulty of approaching saturation [10,11]. Shifting the loop along the x axis so that zero magnetization corresponds to zero field [11] and using $M(\infty) = 4.2 \times 10^5$ A/m, the magnetic hysteresis along [01$\bar{1}$] can be nicely fitted to Eq. (1) with $q = (0.029 \pm 0.001)T^{0.5}$ [red line in Fig. 1(a)]. This value of q as well as the value of H_a are similar to those reported for 90 nm thick Fe_3O_4 (110) film on an MgO substrate [10]. Also in accordance with Sofin *et al.* [10], we find an increase of the q value to $(0.144 \pm 0.019)T^{0.5}$, fitting the magnetization versus magnetic field dependence along the [100] direction [green line in Fig. 1(a)]. Although the fitting curve does not match the low-field data points so well as in the case of the [01$\bar{1}$] direction, it is a good approximation for the values above H_a, confirming that Eq. (1) indeed describes the approach of the magnetization to saturation. On the other hand, it supports us in a determination of the key anisotropy parameters. Thus, taking the H_a value of 0.3 T and the saturation magnetization of 4.2×10^5 A/m,

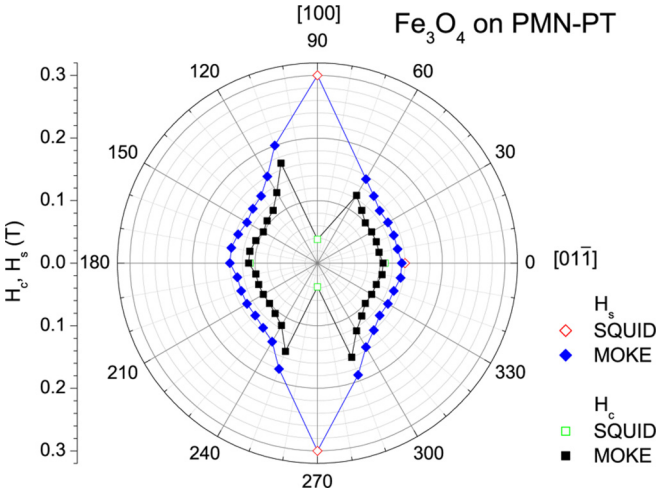

FIG. 2. (Color online) Angular dependence of the coercive field H_c and saturation field H_s, deduced from MOKE and SQUID loops of the Fe_3O_4 film on (011) PMN-PT, showing a [100] hard axis. At 90° and 270° the saturation field equals the anisotropy field. The line is a guide to the eye.

the absolute value of an anisotropy constant, estimated as their product divided by 2 [12,13], is found to be $\sim 6.3 \times 10^4$ J/m^3, while it is only $\sim 1.1 \times 10^4$ J/m^3 in bulk magnetite [14].

For a detailed study of the magnetocrystalline anisotropy, the MOKE technique was used to acquire the magnetization loops, showing an approximately squarelike shape at sample rotation angles from −70° to 60° and from 110° to 250° with respect to the [01$\bar{1}$] direction. Examples of such loops are shown in Fig. 1(b), demonstrating that the coercive field H_c, where the magnetization crosses zero value, and the saturation field H_s, where the hysteresis loop closes and the magnetization is about to saturate, depend on the angle. Analyzing the loops, an angular dependence of H_c is deduced and plotted in Fig. 2. From the angular-dependent magnetometry study of Fe_3O_4 films on (011) PMN-PT, we find that along the [01$\bar{1}$] and equivalent directions (0° and 180°), an H_c of 0.11 T is slightly higher than that of 0.10 T in the minima at around 30°, 150°, 210°, and 330°. Since the loops are squarelike, H_s values are very similar (∼0.03 T higher than H_c). On the other hand, Fig. 2 shows that approaching 90° and 270°, corresponding to the [100] hard-axis and equivalent directions, the field where the magnetization crosses zero value and the field where the hysteresis loop closes are considerably different. H_c approaches zero, while H_s increases toward the anisotropy field of 0.3 T, as determined by the SQUID magnetometry (Fig. 1). Such behavior is in accordance with the Stoner-Wohlfarth model [12] and the factor 3 change of the saturation field when the sample is rotated in-plane shows a strong uniaxial in-plane anisotropy.

In addition to the considerable magnetocrystalline anisotropy in the Fe_3O_4 films epitaxially grown on (011) PMN-PT, leading to a different switching, a strongly anisotropic behavior was also observed in their application-related transport properties. The resistivity along the [01$\bar{1}$] direction ($\sim 2 \times 10^{-2}$ Ω cm at room temperature) was about twice higher than that along the [100] ($\sim 1 \times 10^{-2}$ Ω cm). At the same time, the order of the room-temperature resistivity is

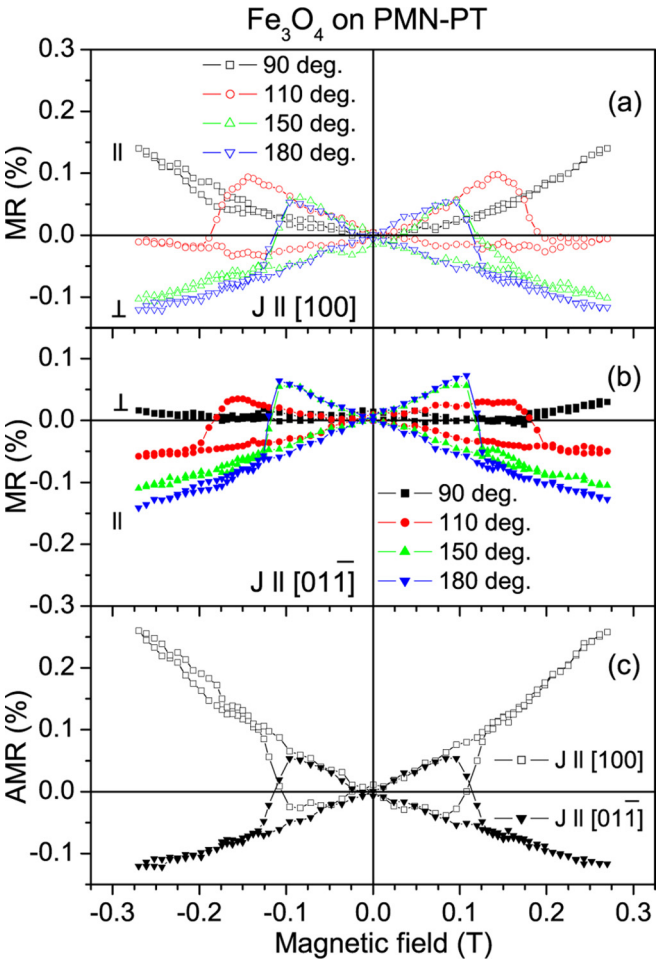

FIG. 3. (Color online) Room-temperature magnetoresistance ratio $\Delta R/R_0$ of the Fe_3O_4 film on poled (011) PMN-PT, measured with the magnetic field applied along the [100] (90°, squares), [01$\bar{1}$] (180°, down triangles), and intermediate directions of 110° (circles) and 150° (up triangles) and current along the [100] (a) and [01$\bar{1}$] (b) in-plane directions. (c) Room-temperature anisotropic magnetoresistance of the Fe_3O_4 film on (011) PMN-PT as function of magnetic field for the currents along the [100] (open symbols) and [01$\bar{1}$] (solid symbols) in-plane directions. The lines are guides to the eye.

comparable to that for the magnetite films deposited on MgO substrates [10,15–17].

The room-temperature magnetoresistance of a Fe_3O_4 film on a poled (011) PMN-PT substrate is shown in Fig. 3 for [100] [Fig. 3(a)] and [01$\bar{1}$] [Fig. 3(b)] current directions and magnetic field along the [100], [01$\bar{1}$], and intermediate in-plane directions as a function of the applied magnetic field H. The MR ratio is defined as

$$\Delta R/R_0 = [R(H) - R(0)]/R(0), \qquad (2)$$

where $R(0)$ denotes the resistance at zero field that is identical within the experimental error for the longitudinal (current and magnetic field directions are parallel) and transverse (current and magnetic field directions are perpendicular) geometry, marked in Figs. 3(a) and 3(b) by the symbols ∥ and ⊥, respectively. These results show that the MR strongly depends on the magnetic field direction, being positive when the

magnetic field is along [100] and negative when it is along [01$\bar{1}$].

As reported in the literature, the magnetite single crystals reveal a moderate MR of anisotropic type, negative in longitudinal and positive in transverse geometry when the current is along the [01$\bar{1}$] direction with the MR value saturating above the anisotropy field when the magnetization is aligned with the applied magnetic field [16]. However, (001)-oriented magnetite films show a considerable negative magnetoresistance along both the [01$\bar{1}$] and [100] directions (in both longitudinal and transverse geometry), depending linearly on the applied magnetic field. This behavior was attributed to carrier transport across antiphase boundaries (APBs) [16,17], the natural growth defects, resulting from the fact that the lattice constant of Fe_3O_4 is more than two times larger than the one of the substrate. The simplest approximation for the spin configuration at the APB (which is likely to be much more complex) is a row of spins that, except for one spin, are ferromagnetically ordered; i.e., the magnetic coupling over a large fraction of these boundaries is antiferromagnetic (AF). Upon application of a magnetic field, the AF spins will align themselves to some degree with the magnetic field, thus increasing the electron transport across the boundaries [17]. However, the AF exchange coupling at the APBs is so strong that a complete alignment and hence saturation of the MR is not achievable in magnetic fields up to 5 T at least [17]. On the other hand, in the magnetite films epitaxially grown on (110) MgO substrates, an orientation-dependent low-field longitudinal MR was observed, being negative in the [01$\bar{1}$] direction but positive in the [100] direction [10]. The positive MR was ascribed to the domain wall magnetoresistance due to the reduction in the width of the canted spin structure around APBs and associated increase in the spin canting [10].

The MR behavior observed in our Fe_3O_4 films on a (011) PMN-PT substrate is also different from the (001)-oriented films. When the magnetic field is along the [100] direction, corresponding to 90° curves in Figs. 3(a) and 3(b), a positive MR with nonlinear dependence on the magnetic field is detected. A drastically different MR behavior is observed for the magnetic field along the orthogonal in-plane [01$\bar{1}$] direction, corresponding to 180° curves in Figs. 3(a) and 3(b). The MR along the [01$\bar{1}$] direction first linearly increases, but reaching the magnetic fields corresponding to the switching fields found by the magnetometry measurements (the irreversible switching fields are for the most directions equal to the H_c values) it shows switching downwards. Above this switching field, the MR is negative, resembling the one measured with in-plane fields on Fe_3O_4 films and ascribed to APBs [16]. Thus, in our strongly anisotropic magnetite films, APBs give a considerable response to the negative MR when magnetic field is along [01$\bar{1}$] but they are not detectable for the field along the [100] hard axis. Additionally, Figs. 3(a) and 3(b) show that, when the magnetic field is along directions intermediate between [01$\bar{1}$] and [100], the MR continuously transforms from the behavior characteristic for APBs to the one characteristic for anisotropic MR (AMR), although the change is more gradual in the vicinity of [01$\bar{1}$] direction and it is more abrupt close to the [100] direction. Moreover, during this transformation

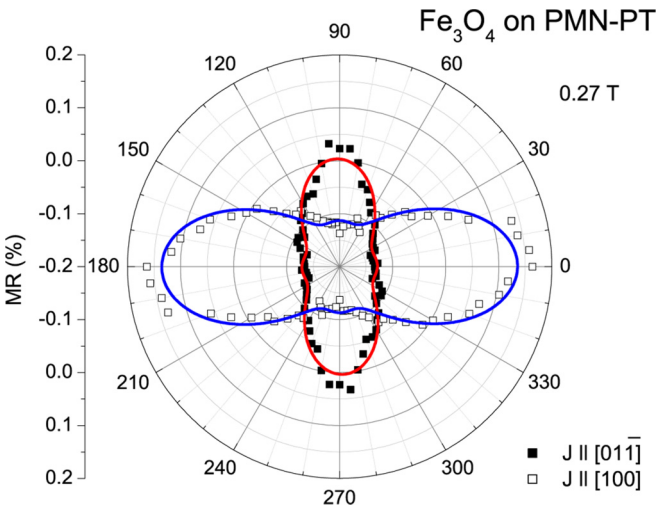

FIG. 4. (Color online) Room-temperature magnetoresistance ratio $\Delta R/R_0$ at a magnetic field of 0.27 T for [100] (open symbols) and [01$\bar{1}$] (solid symbols) current directions as a function of angle between the current and magnetic field, deduced from the magnetic field dependencies of the MR in the Fe_3O_4 film on (011) PMN-PT at different angles. The solid lines are fits to Eq. (4) with $n = 2$.

the switching field changes in agreement with the angular dependence presented in Fig. 2.

The AMR is usually defined as a ratio

$$\mathrm{AMR} = [R_{\mathrm{long}} - R_{\mathrm{trans}}]/[R_{\mathrm{long}}/3 + 2R_{\mathrm{trans}}/3], \qquad (3)$$

where R_{long} and R_{trans} are the resistances for magnetic field applied parallel and perpendicular to the current direction, respectively [15]. So using the data presented in Figs. 3(a) and 3(b) we could deduce the magnetic field dependence of the AMR in the Fe_3O_4 film on (011) PMN-PT for the currents along the [100] and [01$\bar{1}$] in-plane directions. Above ∼0.1 T, the AMR is positive for the [100] direction and negative for the [01$\bar{1}$] direction. At room temperature and a magnetic field of 0.27 T, the AMR value is about −0.12% for the [01$\bar{1}$] and about 0.26% for the [100] current direction, in agreement with earlier reports [15,16]. Particularly, a room-temperature AMR of about −0.2% along the [01$\bar{1}$] and about 0.5% along the [100] direction at a magnetic field of 1 T were reported for films studied by Ziese and Blythe [16].

Figure Figure 4 shows the dependence of the magnetoresistance of the Fe_3O_4 film on poled (011) PMN-PT at a magnetic field of 0.27 T on the angle between the current and magnetic field directions for both [100] and [01$\bar{1}$] current directions. These results are deduced from the from the magnetic field dependences of the MR at different angles. For both [100] and [01$\bar{1}$] current directions, the MR varies periodically with a period of 180°. However, the amplitude of the variation depends on the current direction. For the current along the [01$\bar{1}$] direction it is smaller and MR is mainly negative, besides the vicinity of 90° (270°), whereas for the current along the [100] direction the angular dependence of the MR is stronger, showing comparable positive and negative contributions.

The field rotation is performed in a (011) plane, for which the angular dependence of MR obtained from symmetry arguments for both [100] and [01$\bar{1}$] current directions [13]

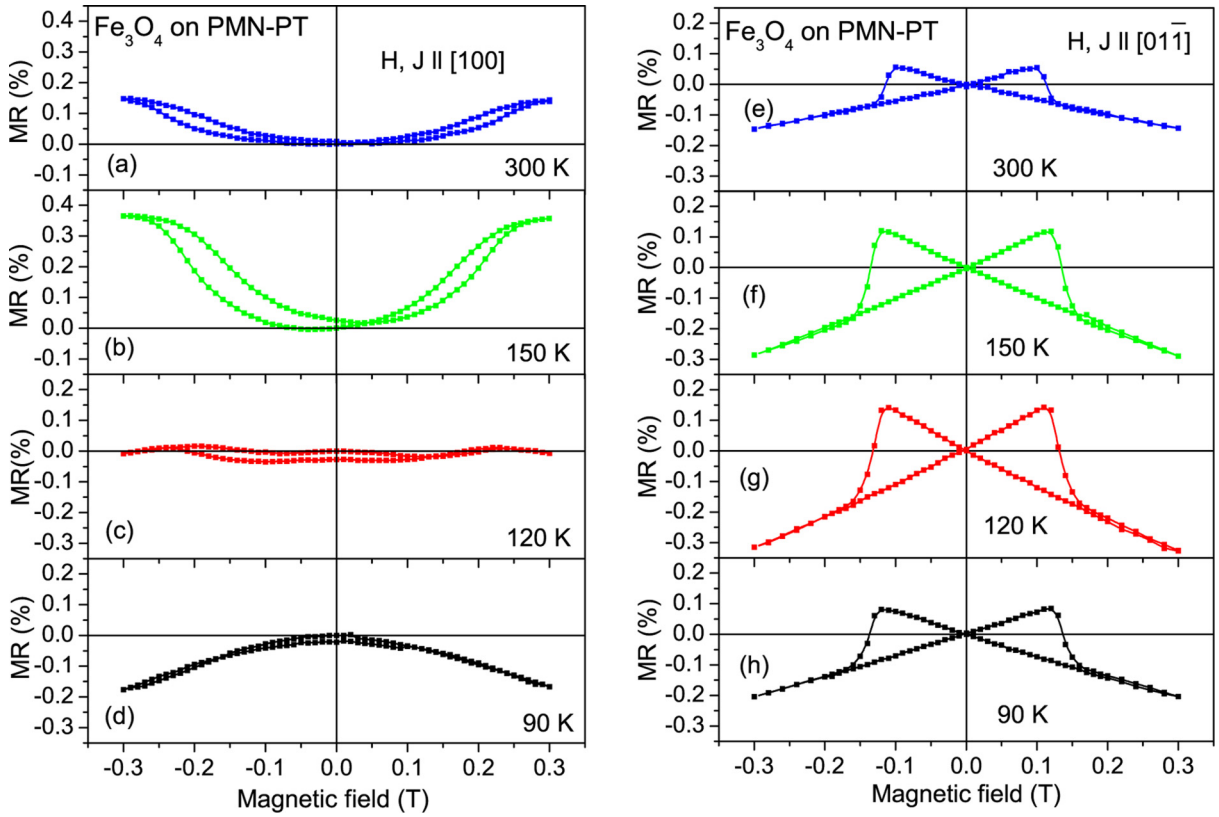

FIG. 5. (Color online) Magnetoresistance ratio $\Delta R/R_0$ of the Fe_3O_4 film on poled (011) PMN-PT, measured at 300 K [(a), (e)], 150 K [(b), (f)], 120 K [(c), (g)], and 90 K [(d), (h)] with applied magnetic field and current along the [100] [(a)–(d)] and [01$\bar{1}$] [(e)–(h)] in-plane directions. The lines are guides to the eye.

should follow

$$\Delta R/R_0 = c_0 + \sum_{n=1}^{\infty} c_{2n} \cos 2n\theta, \tag{4}$$

where c_0 and c_{2n} are the fitting coefficients and θ is the angle between the magnetic field and current directions. Limiting to $n = 1$ that corresponds to a twofold symmetry of the angular MR response [18], we could fit our results but with R^2 values quite far from 1, being only 0.841 and 0.888 for the [01$\bar{1}$] and [100] current directions, respectively. The R^2 values were considerably improved (to 0.943 and 0.968) when the data were fitted to Eq. (4) with $n = 2$, implying the contribution of the fourfold symmetry in addition to the twofold symmetry. Thus, the fourfold symmetry is detectable at room temperature in our magnetite films epitaxially grown on (011) PMN-PT, while such contribution was observed for the (001)-oriented Fe_3O_4 films only on cooling below 200 K and related to the polaron formation [15,19,20]. No such report on the angular dependence of MR is known to us so far on the Fe_3O_4 films on (011) substrates.

Next, we have carried out transport measurements at different temperatures across the Verwey transition down to 90 K, as presented in Fig. 5 for longitudinal MR of the Fe_3O_4 film on poled (011) PMN-PT. For the [100] direction [Figs. 5(a)–5(d)], the MR is found to be positive in the magnetic field up 0.3 T only above ~120 K, while on cooling below this temperature the magnetite film shows negative MR. Similar MR behavior in the [001] direction was observed on the magnetite films grown on (110) MgO substrates [10]. Positive MR was ascribed to the domain walls along APBs, while its vanishing below T_V was related to the hard axis to easy axis transition in the [100] direction [10]. For the Fe_3O_4 films on (001) MgO substrates, the AMR was found to change sign near T_V in agreement with the sign change of the magnetic anisotropy constant K_1 at the Verwey transition [16]. The T_V of ~120 K observed in our samples thus confirms the high quality of the magnetite films epitaxially grown on (011) PMN-PT. For the [01$\bar{1}$] direction [Figs. 5(e)–5(h)], the shape of the MR dependence on the magnetic field stays the same in all the temperature range studied, revealing just a slight increase of the switching field upon cooling from 300 to 200 K and an increase of the MR value at 0.3 T from ~0.15% at 300 K to more than 0.3% around the T_V.

Finally, we investigate the effects of strain on the Fe_3O_4 thin-film properties. Figure 6 shows the effect of poling the (011) PMN-PT substrates on the MR of the magnetite films, measured with about 10° in-plane rotation to the [100] and [01$\bar{1}$] directions at fields up to 0.3 T. While the MR behavior is similar for both unpoled and poled states between 300 K [Figs. 6(a), 6(e)] and 150 K [Figs. 6(b), 6(f)], a considerable change in MR is observed when the sample is cooled to and below T_V [Figs. 6(c), 6(d), 6(g), 6(h)]. For the direction close to [100] [Figs. 6(a)–6(d)], a strong decrease of the MR with poling from 0.63% to 0.14% at 0.3 T is evident, being in qualitative agreement with results reported for the [100] direction by Liu *et al.* and related to increase of the magnetic anisotropy of Fe spins in the vicinity of the APBs induced by

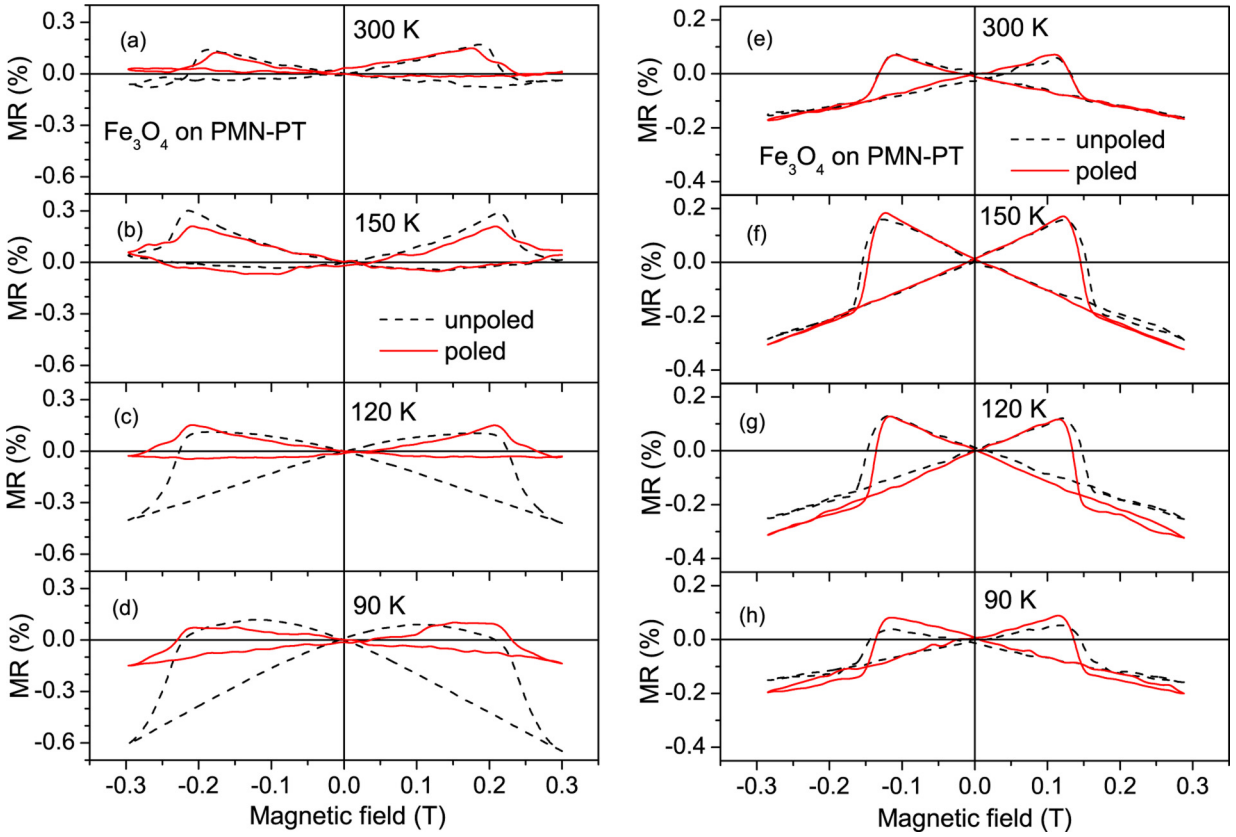

FIG. 6. (Color online) Magnetoresistance ratio $\Delta R/R_0$ of the Fe_3O_4 film on (011) PMN-PT as a function of magnetic field applied together with current along the direction rotated in-plane by about 10° from the [100] [(a)–(d)] and [01$\bar{1}$] [(e)–(h)] axes, measured at 300 K [(a), (e)], 150 K [(b), (f)], 120 K [(c), (g)], and 90 K [(d), (h)] before (dashed black line) and after poling (solid red line) of the piezosubstrate.

the strain [8]. On the other hand, for the direction close to [01$\bar{1}$] [Figs. 6(e)–6(h)], a slight increase of the MR from 0.15% to 0.20% at 0.3 T is detected, which shows the strong coupling between the magnetotransport and the electronic properties.

IV. CONCLUSIONS

In conclusion, magnetization and magnetotransport properties of Fe_3O_4 films epitaxially grown on (011) PMN-PT piezosubstrates were systematically investigated as a function of crystallographic orientation and strain. Angular dependence of the magnetization loops studied for (011) Fe_3O_4 films at room temperature shows a significant in-plane magnetocrystalline anisotropy with [100] being the hard axis. Along this direction, the magnetization loops are slanted whereas along the [01$\bar{1}$] direction ±70° the loops are square shaped, clearly revealing the presence of a ferrimagnetic state. Room-temperature magnetotransport measurements as a function of angle between the current and magnetic field allow us to detect the fourfold symmetry and to conclude that antiphase boundaries in our strongly anisotropic magnetite films should be strictly oriented along the [01$\bar{1}$] direction, giving no significant negative contribution to MR at a magnetic fields along [100]. The variation of longitudinal MR with temperature is found to be different in the [100] and [01$\bar{1}$] directions as well. Whereas the longitudinal MR sign is permanently negative above the switching field for [01$\bar{1}$], similarly to that commonly observed for (100)-oriented Fe_3O_4 films and related to the presence of antiphase boundaries, the sign of the MR along [100] changes from positive to negative around the Verwey transition temperature on cooling. When we pole the PMN-PT piezosubstrate, we find that the MR response of the magnetite film was strongly affected in particular in the vicinity of the Verwey transition, showing that we can tailor the magnetic properties by strain induced by electric fields. Furthermore, the changes of the magnetotransport properties at the Verwey transition demonstrate the strong correlation between the MR and the phases present below and above T_V.

ACKNOWLEDGMENTS

Lambert Alff is acknowledged for the initiative to study the change of magnetic behavior across the Verwey transition of magnetite thin films provided by his group. This work was funded by the EU's 7th Framework Program IFOX (NMP3-LA-2010 246102), the Graduate School of Excellence MAINZ (GSC 266 Mainz), the German Science Foundation (DFG), and the ERC (2007-Stg 208162). A.T. acknowledges also funds by FEDER through Programa Operacional Factores de Competitividade–COMPETE and national funds through FCT–Fundação para a Ciência e Tecnologia within the CICECO project FCOMP-01-0124-FEDER-037271 (FCT Ref. PEst-C/CTM/LA0011/2013) and independent researcher grant IF/00602/2013.

[1] C. A. F. Vaz, J. Hoffman, C. H. Ahn, and R. Ramesh, Adv. Mater. **22**, 2900 (2010).
[2] S. Finizio, M. Foerster, M. Buzzi, B. Krüger, M. Jourdan, C. A. F. Vaz, J. Hockel, T. Miyawaki, A. Tkach, S. Valencia, F. Kronast, G. P. Carman, F. Nolting, and M. Kläui, Phys. Rev. Appl. **1**, 021001 (2014).
[3] L. R. Bickford, J. Pappis, and J. L. Stull, Phys. Rev. **99**, 1210 (1955).
[4] F. Walz, J. Phys.: Condens. Matter **14**, R285 (2002).
[5] O. Noblanc, P. Gaucher, and G. Calvarin, J. Appl. Phys. **79**, 4291 (1996).
[6] T. Wu, P. Zhao, M. Bao, A. Bur, J. L. Hockel, K. Wong, K. P. Mohanchandra, C. S. Lynch, and G. P. Carman, J. Appl. Phys. **109**, 124101 (2011).
[7] M. Liu, O. Obi, J. Lou, Y. Chen, Z. Cai, S. Stoute, M. Espanol, M. Lew, X. Situ, K. S. Ziemer, V. G. Harris, and Nian X. Sun, Adv. Funct. Mater. **19**, 1826 (2009).
[8] M. Liu, J. Hoffman, J. Wang, J. Zhang, B. Nelson-Cheeseman, and A. Bhattacharya, Sci. Rep. **3**, 1876 (2013).
[9] M. Baghaie Yazdi, M.-L. Goyallon, T. Bitsch, A. Kastner, M. Schlott, and L. Alff, Thin Solid Films **519**, 2531 (2011).
[10] R. G. S. Sofin, S. K. Arora, and I. V. Shvets, Phys. Rev. B **83**, 134436 (2011).
[11] S. Geprags, D. Mannix, M. Opel, S. T. B. Goennenwein, and R. Gross, Phys. Rev. B **88**, 054412 (2013).
[12] E. C. Stoner and E. P. Wohlfarth, Philos. Trans. R. Soc. A **240**, 599 (1948).
[13] M. Ziese, I. Vrejoiu, and D. Hesse, Phys. Rev. B **81**, 184418 (2010).
[14] L. R. Bickford, Phys. Rev. **78**, 449 (1950).
[15] R. Ramos, S. K. Arora, and I. V. Shvets, Phys. Rev. B **78**, 214402 (2008).
[16] M. Ziese and H. J. Blythe, J. Phys.: Condens. Matter **12**, 13 (2000).
[17] W. Eerenstein, T. T. M. Palstra, S. S. Saxena, and T. Hibma, Phys. Rev. Lett. **88**, 247204 (2002).
[18] M. Bibes, V. Laukhin, S. Valencia, B. Martinez, J. Fontcuberta, O. Yu. Gorbenko, A. R. Kaul, and J. L. Martinez, J. Phys.: Condens. Matter **17**, 2733 (2005).
[19] N. Naftalis, A. Kaplan, M. Schultz, C. A. F. Vaz, J. A. Moyer, C. H. Ahn, and L. Klein, Phys. Rev. B **84**, 094441 (2011).
[20] H.-C. Wu, R. Ramos, R. G. S. Sofin, Z.-M. Liao, M. Abid, and I. V. Shvets, Appl. Phys. Lett. **101**, 052402 (2012).